Optical Calibration of the FUV Spectrographic Imager for the IMAGE Mission

Serge Habraken*, Yvette Houbrechts, Etienne Renotte, Marie-Laure Hellin, Anne Orban, Pierre Rochus (a)
Stephen Mende, Harald Frey, Steve Geller, and Joe Stock (b)

(a) Centre Spatial de Liège, B-4031 Angleur (Belgium)
(b) Univ. of California Berkeley, Space Sciences Lab., CA

ABSTRACT

The FUV Spectrographic Imager for IMAGE is simultaneously imaging auroras at 1218 and 1358 Å. It is designed to efficiently reject the Lyman-α emission line at 1215.7 Å.
This paper describes the optical calibration. The content is :
a. Field of View calibration : detector pixels location with respect to the reference optical cube; distortion matrix used to compute the TDI (compensation of the satellite spin).
b. Radiometric calibration : detector response and linearity; instrument throughput according to its clear aperture and mirror reflection lost; response vs. wavelength and band-rejection certification.

Keywords: Spectrograph, optical calibration, aurora observation, FUV optics.

1. INTRODUCTION

1.1. Overview of the mission requirements

The FUV system is an experiment which forms part of the instrument package of the IMAGE program, a NASA/MIDEX mission due for launch in early 2000. The FUV system consists of four major subassemblies, namely, a Spectrographic Imager (SI), a Wideband Imaging Camera (WIC), a geocorona (and sun) sensor, and a Main Electronic Package (MEP).
This paper is focused on the optical calibration of the Spectrographic Imager. The optical design was described in a previous paper[1]. Alignment and optical performances were part of another paper[2]. The mechanical design and verification (space qualification) were described too[3].
Briefly, science requirements driving FUV SI design are :
(1) to image the entire aurora oval from a spinning spacecraft at 7 earth radii apogee altitude;
(2) to separate spectrally the statistical noise of the intense cold geocorona (Lyman-α emissions at 1216 Å) from the hot proton precipitation (Doppler shifted Lyman-α emissions), and the 1200 Å emission;
(3) to separate spectrally the electron (1304 and 1356 Å) and proton (1216 Å) auroras.
First requirement involves a large field of view (FoV) : 15° x 15°.
Second requirement gives rise to a high spectral resolution, better than 2 Å. The Doppler shifted Lyman-α signal to be detected is about 100 times less intense than the Lyman-α geocoronal emissions at 1216 Å.
Third requirement means that the 1356 Å signal must be isolated from the 1304 Å signal.
Nitrogen emissions near 1200 Å (triplet lines at 1199.55, 1200.22, and 1200.71 Å) have also to be filtered out.
The spatial resolution requirement specifies that, from 7 earth radii, the aurora oval shall be imaged with a 90 km × 90 km resolution. The related angular resolution is about 7 arcmin x 7 arcmin i.e. 128 pixels x 128 pixels.

1.2. Brief description of the SI optical system

Since full descriptions of the optical design and performances are already published[1,2], only a summary of the main characteristics will be given.
Figure 1 shows a ray-tracing at 1218 and 1356Å including the zero and +1 diffraction orders only (for clarity).
The instrument consists of two main optical subsystems : a monochromator, and a "twin" back-imager (one at 1218 Å, the other one at 1356 Å).
The monochromator is designed to produce the largest dispersion, in order to reach the required high spectral resolution. Focal length is 500 mm and the grating ruling is 3600 lp/mm (holographic recording). The grating curvature is spherical; the

Part of the SPIE Conference on EUV, X-Ray, and Gamma-Ray Instrumentation for Astronomy X
Denver, Colorado • July 1999 SPIE Vol. 3765 • 0277-786X/99/$10.00

collimator curvature is hyperbolic. The linear spectral dispersion is about 182 µm/Å in the exit slit plane. As depicted in figure 1, a first image of the earth is produced approximately at the grating plane. The aim of the back-imager is to relay this image after diffraction by the grating, in order to obtain two spectrally separated images. Each sub-assembly of the back-imager is a two-mirror optical system. The first mirror is spherical. The second one is conical (elliptical) and off-axis. A flat folding mirror is added to the 1356 Å imager in order to allow fitting the two detectors in close proximity. Detectors are Crossed-delay-line MCP[4].

The slit configuration is made of a grill with 9 parallel slits, designed to stop the 1200 and 1216 Å (1215.67 Å) lines, simultaneously. The slit spacing (period) is determined for this purpose : 5.223 Å i.e. one third of the wavelength difference between the two lines.

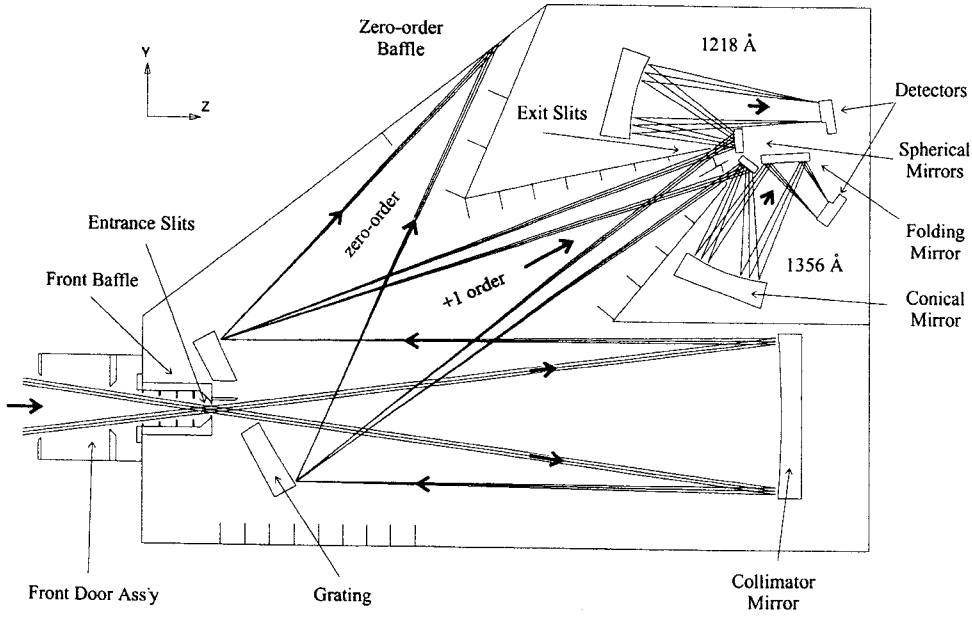

Figure 1 : Ray-tracing at 1218 and 1356Å including the zero and +1 diffraction orders.

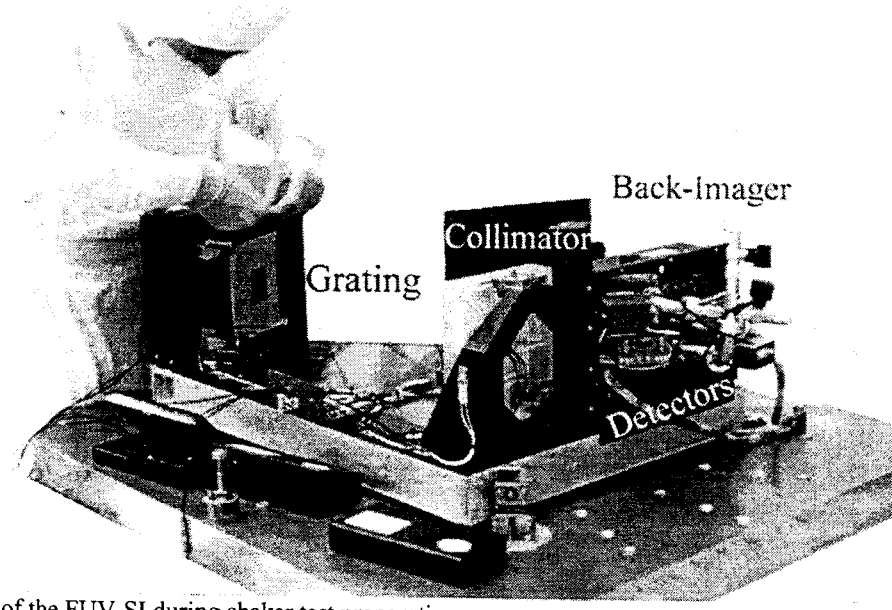

Figure 2 : Picture of the FUV-SI during shaker test preparation

2. FIELD OF VIEW CALIBRATION

2.1. Principle

IMAGE is a spinning spacecraft. For that reason, several instruments need to use a TDI mode (Time-Delay Integration). In order to work properly, the TDI device need :
- a look-up table adjusted with respect to the image distortion,
- a good knowledge of the S/C spinning axis with respect to the image.

The first requirement is performed by measuring the distortion matrix of the instrument and calculating a polynomial fitting. The second requirement is reached by measuring the FoV with respect to the reference optical cube mounted on the instrument. Later, the orientation of the cube will be determined with respect to the S/C axis referential (S/C reference cube and estimated spinning axis).
That is summarizing the concept of the field of view calibration.
The instrument is mounted on a 2-axis rotation stage which allows for simulating the illumination over the whole FoV (15° x 15°). Measurement are performed inside a vacuum chamber (1.5 m dia.). The collimated beam is generated by a discharge lamp mounted on a UV monochromator and a collimating mirror aligned with the focal point on the exit slit of the monochromator (not actually a slit but a pinhole).
Figure 3 shows a picture of the (open) FUV-SI and the rotation stage installed inside the chamber (not shown for clarity).

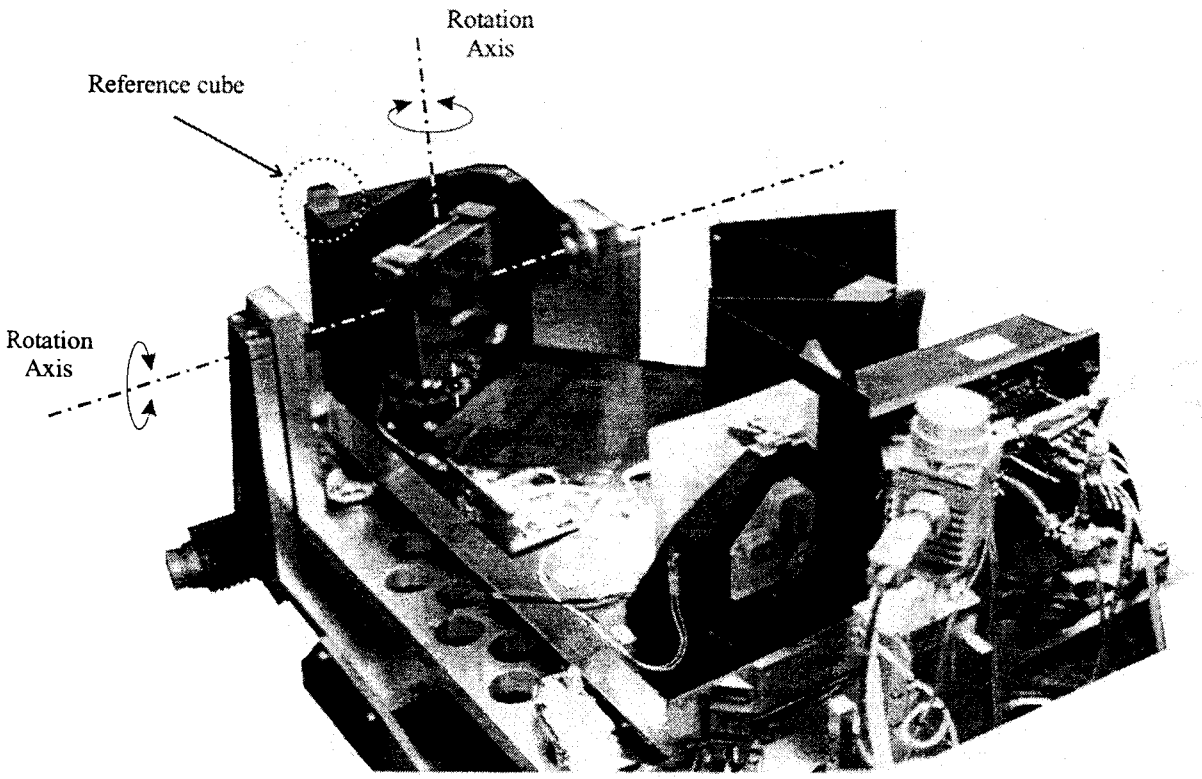

Figure 3 : Picture of the FUV-SI mounted on a vacuum compatible rotation stage

The calibration was performed in two main steps :
1. Under vacuum, measurement of spot image location on flight model detectors for various shooting angles using a collimated FUV beam (angles were determined by motor steps pre-calibration).
2. Accurate determination of the shooting angles with respect to the reference cube using theodolite.

The first step was performed with 32 lines of sight inside the FoV for both wavelength channels (1218/1356 Å). It includes the determination of the image borders (extremes and central hole).
The second step required to shoot the cube with a theodolite. Since the instrument is inside a vacuum chamber with a top cover, the cube is not directly accessible. The removal of the vacuum chamber lateral ring-envelope was decided in order to keep the rotation stage accurately on the same configuration as it was during the vacuum test and having the cube on the line of sight of a theodolite. The detailed procedure was not straightforward :

- A large mirror is mounted in front of the SI entrance aperture and aligned with respect to the front face of the cube.
- A visible collimated beam is generated by replacing the UV lamp with a HeNe laser in front of the entrance slit of the monochromator (adequately tuned). The rotation stage is moved until the mirror is precisely back reflecting the collimated beam.
- Shooting the cube laterally (under grazing incidence) allows for determining the orientation of the cube with respect to the ground reference (absolute horizontal). That is denoted by γ on figure 4.
- The theodolite (shooting next the front face of the cube) was mounted with the same deviation from the absolute horizontal (γ).
- Finally, the rotation axis was actuated to return at the locations used during the vacuum measurement and the angle of incidence was determined with respect the reference cube axis only (absolute referential, not related to external axis).

The correlation of the point spread function centroid and the measured angle by theodolite is the input of the distortion matrix and was used to find a polynomial fitting of the image distortion.

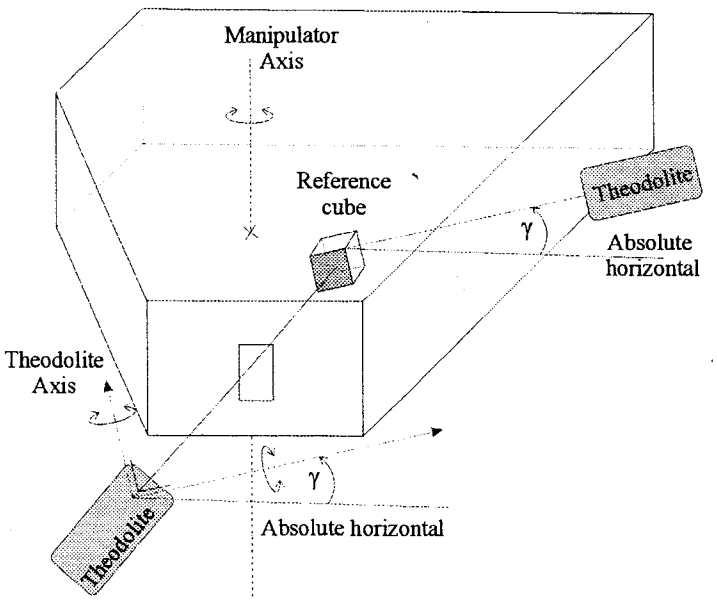

Figure 4 : Schematic drawing of the theodolite alignment and measurement.

2.2. Results

The angular error over the full procedure is estimated at about 20 arcsec RMS. That is far better than the requirement, since the specified angular resolution of the SI is 7 arcmin.
The present FoV is slightly larger than the specified value 15° x 15°. Central hole and borders are determined at both wavelength channels. The final imaging quality was determined; the Full-Width Half-Maximum (FWHM) is :

100 µm ± 20 µm at 1218 Å and 95 µm ± 10 µm at 1356 Å

The resulting angular resolution is about 5 arcmin x 5 arcmin.

A set of two second-order polynomial fitting was calculated : one fitting per wavelength channel.
The RMS distortion fitting error is about 30 µm (1.4 arcmin i.e. 1/5th of the specified resolution).
This result is in agreement with the TDI requirement. No significant image degradation should be encountered from the TDI correction with look-up tables.

3. RESPONSE CALIBRATION

3.1. Principle

The aim of that test consists in the measurement of the response of the spectrograph versus the wavelength. Response variations over the FoV has to be estimated too.
Measurements made on mirror samples during manufacturing and acceptance tests already allow for throughput predictions.
The transmission loss through the SI optics can be summarized this way :

- Mirror reflectivity : about 70 %
- Grating diffraction efficiency : about 60 % (coating reflectivity to be additionally taken into account).
- Theoretical transmission through the exit slits : about 90 % at 1218.3 Å and 100 % at 1356 Å.
- 4 reflections are encountered at 1218 Å and 5 reflections at 1356 Å.
- detector window (MgF_2) transmission : about 50% at 1218 Å and 70% at 1356 Å.

The overall resulting transmission is about 7% at 1218.3 Å and 1356 Å.
The last loss factor is the detector photocathode Quantum Efficiency (QE).

Figure 5 depicts the set-up used to perform the calibration.

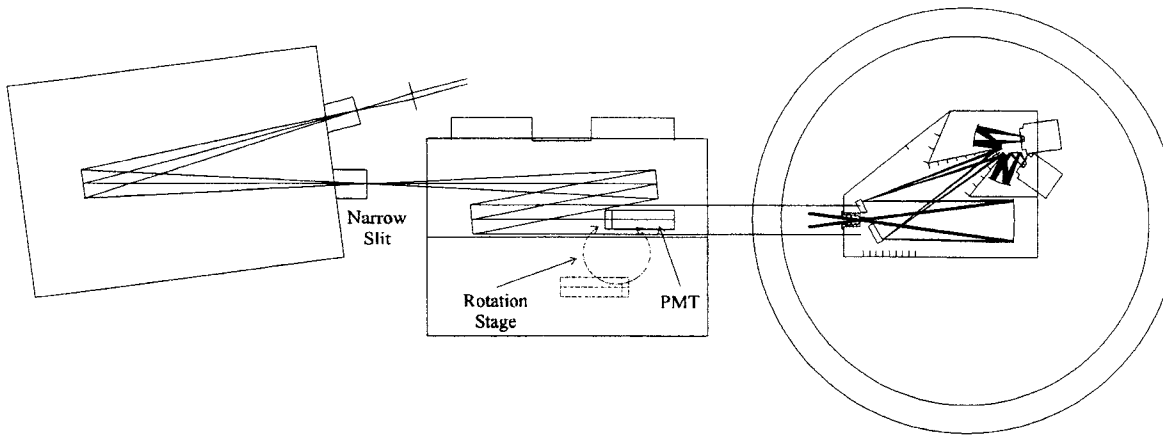

Figure 5 : Set-up for the response calibration test.

The first step consists in calibrating the irradiance reaching the entrance slits of the SI.
The lamp is a discharge lamp filled with Ar which produces a continuum with O and H emission lines, probably due to water residue in the plasma chamber.
The McPherson monochromator is tuned to 2 Å spectral resolution.
A PMT is used on the collimated monochromatic beam. Its aperture size is fitting the SI entrance slit rectangle (36 mm x 9 mm); its position is adjusted to be on the line of sight of the entrance slit grill.
Using the correction of the PMT response (QE) and surface, the entrance irradiance on the SI slit grill is measured (photons/s/cm² based on counts/s) at each wavelength (within a spectral bandwidth of 2 Å).
The next step consists in rotating the PMT out of the collimated beam. The FUV-SI is now fully illuminated and the SI detector count rate is measured.
The SI response definition can now be proposed :

SI response = effective SI detector count rate / entrance irradiance

The SI response at a given wavelength is the expected effective count rate when the entrance irradiance (inside the FoV) is 1 photon/s/cm². The effective count rate is defined by the count rate subtracted with the detector noise.

Response variation over the FoV is realized by the same procedure but wavelength centered at 1218.3 and 1356 Å (response maximum). The aim is to determine the spatial distribution of response for a mapping of 24 field angles.
Reasons why response is depending on the FoV are listed below :

- Detector flat field pattern is not uniform
- Mirror coating are not uniform and reflectivity depends on the angle of incidence.
- Grating diffraction efficiency is not uniform and also depends on the angle of incidence.
- Vignetting may occur at FoV extremes.

3.2. Results

Results discussed below show the full spectral analysis for a single field angle inside the FoV of the SI. Both wavelength channels were scanned :

- 1170-1270 Å bandwidth
- 1300-1400 Å bandwidth

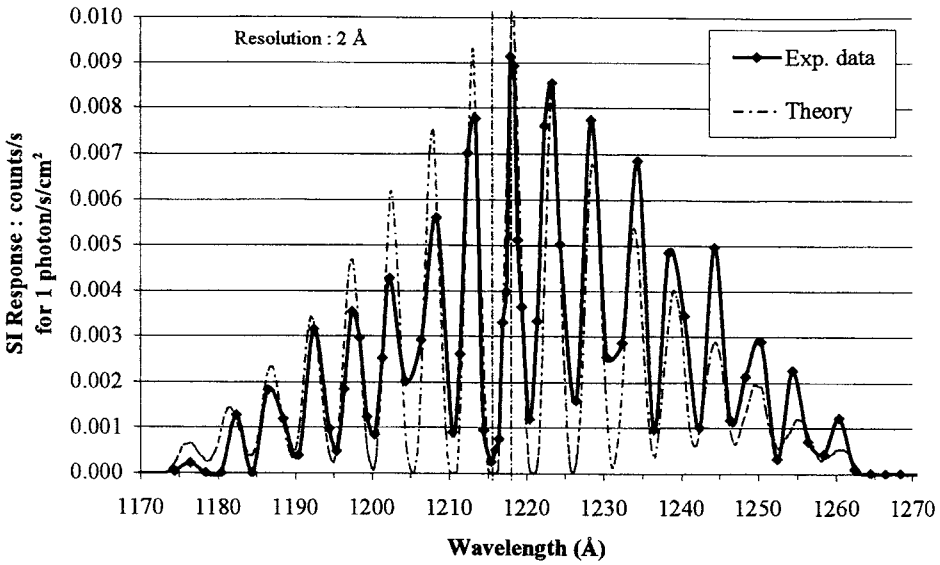

Figure 6 : Comparison between theoretical and experimental SI Response on the 1218 Å channel. The theoretical max is arbitrary.

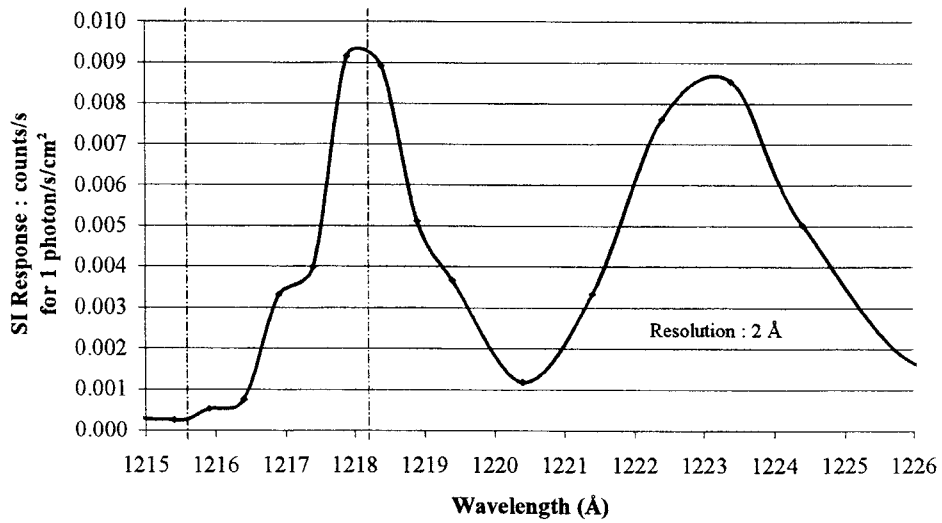

Figure 7 : SI Response on the 1218 Å channel. Spectral resolution is 2 Å. The bandwidth is expanded on the Lyman-α and Doppler-shifted Lyman-α region (proton-aurora band)

Figures 6 and 7 depict the response of the first channel. Figure 6 provides an interesting comparison between the theoretical response through the slit grill (9 parallel slits) and the experimental data. Figure 7 is zooming on the Lyman-α bandwidth.

In order to analyze those results, it is necessary to keep in mind that the spectral resolution of the monochromator was tuned to 2 Å. Figure 6 and 7 slightly suffer from that lack of spectral resolution. Indeed, the slit spacing is about 5.2 Å. Anyway, the side lobes are defined. However, we can expect a lack of accuracy in determining the minima and maxima, since the beam is 2 Å wide and the profile is never flat over 2 Å. So, a convolution takes place, resulting in a loss of contrast. It means that we can legitimately expect the minima to be lower and the maxima to be higher...
For a clear comparison between the measured response and the theoretical profile in the 1170-1270 Å region, the theoretical response max was adjusted for best fitting in Figure 6. We see a very good correlation between theoretical and experimental side lobes wavelength. It proofs the precise manufacturing and fine alignment of the slit grill.
The response is maximum around 1218-1218.5 Å. This is in perfect agreement with the instrument requirements. The experimental results shows a response of 9 counts/s with an irradiance of 1,000 photons/s/cm^2.
The ratio between the 1200 Å sensitivity and the sensitivity max (@1218.3 Å) is 10 %
The ratio between the 1215.7 Å (Lyman-α) sensitivity and the sensitivity max (@1218.3 Å) is 6 %. That value has to be compared with the accurate measurement made during the alignment of the SI [2]. The ratio was 1.3% only.
Another major source of error, close to Lyman-α, is coming from the lamp spectrum : the spectrum has a significant increase at Lyman-α. Despite of the fact that it is very convenient for calibrating the monochromator wavelength, it is a major source of error. The PMT is counting photons with the 2 Å resolution. The SI is selecting a more narrow bandwidth which will be counted by the SI detector. For instance, when the monochromator is tuned to 1217 Å, the PMT is still partially counting photons at Lyman-α. Since the spectrum depicts a peak at Lyman-α, it contributes to a major increase of count rate on the PMT but not on the SI.
Figure 8 shows the optical transmission through the monochromator sub-assembly of the SI. Those measurements were performed during the alignment of the instrument [2]. They were obtained by translating the entrance slit in front of a monochromatic H-lamp (an arithmetical conversion between linear translation and wavelength scanning were applied, using the monochromator linear dispersion relationship). For that reason, those data are not attached to the spectral resolution of any external monochromator. They are very accurate, within the translation stage accuracy.

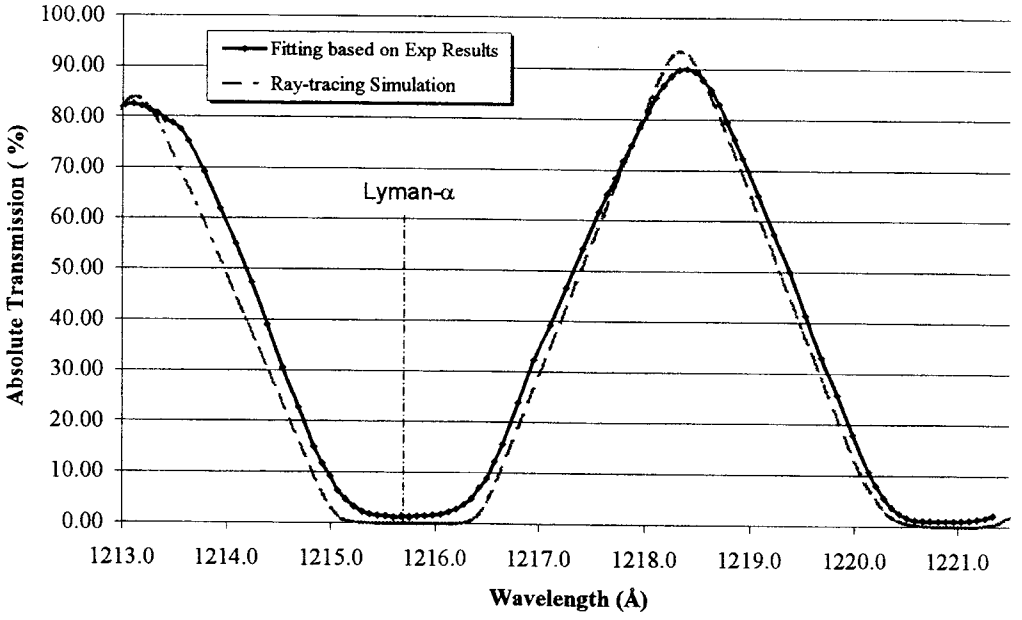

Figure 8 : Comparison between theoretical transmission spectrum of the Wadsworth monochromator (Simulation performed by ray-tracing) and experimental results obtained during the alignment [2].

As pointed above, figure 8 shows the theoretical transmission spectrum based on ray-tracing compared with the measured transmission. The only significant difference is the minimum lobes that never perfectly reach zero on experimental results. As mentioned above, the ratio between the transmission minimum (at Lyman-α) and maximum reached 1.3%. It demonstrates, better than figure 7, how the instrument is performing the Lyman-α rejection and transmits the Doppler-shifted wavelength around 1218 Å. The reason why figure 7 do not predict a satisfactory rejection is mainly the spectral resolution of the measurement performed during the response calibration test.

Figure 9 shows the SI response measurement inside the 1300-1400 Å bandwidth.

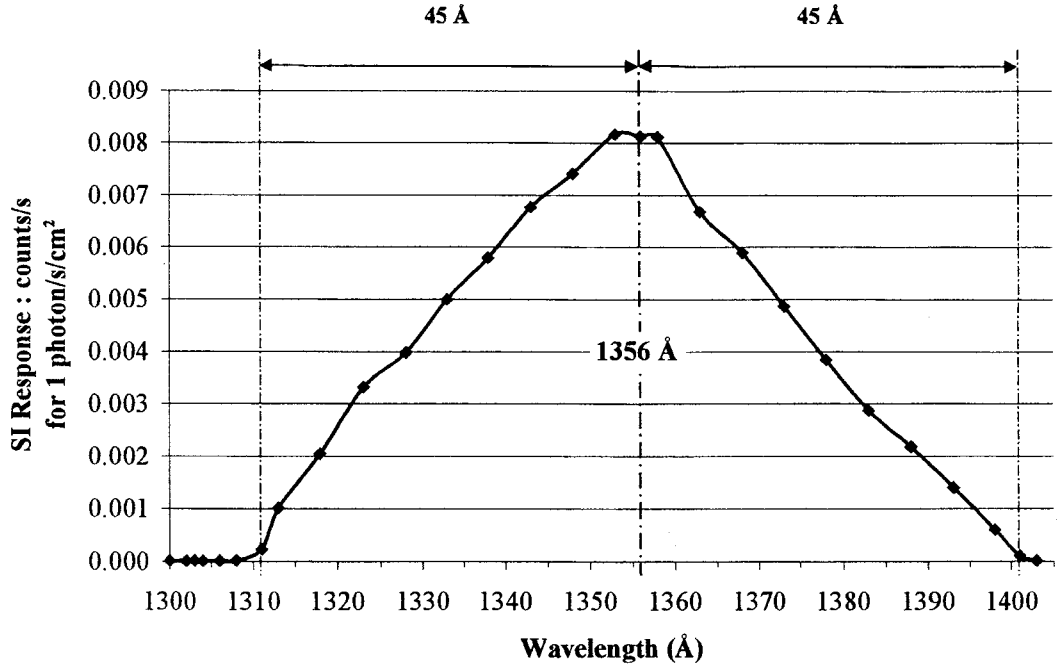

Figure 9 : SI Response on the 1356 Å channel. spectral resolution is 2 Å

The response curve is symmetrical and centered at 1356 Å (maximum around 1356 Å). This is in perfect agreement with the instrument requirements. The experimental results shows a response of 8 counts/s with an irradiance of 1,000 photons/s/cm². The 1302 and 1304 Å and the LBH bands ($\lambda > 1400$ Å) are efficiently rejected :
- the ratio between the 1302-1304 Å sensitivity and the sensitivity max (@1356 Å) is only 0.1 %
- the ratio between the 1401 Å sensitivity and the sensitivity max (1356 Å) is 1.35 % but is decreasing to 0.16 % at 1403 Å.

Among the additional sources of errors introduced during the response calibration test, we can mention the following :
- The monochromator wavelength tuning is calibrated thanks to the Lyman-α line and the doublet line at 1302-1304 Å. The residual error is estimated to ±0.25 Å on the first channel (1218) and ±0.5 Å on the second channel (1356).
- The positioning of the PMT, on the line of sight of the entrance slit grill is estimated to ±0.5 mm. Since the beam intensity distribution is not uniform, it can generate an error, especially on the wavelength axis.

The response variation over the FoV is shown in figures 10 and 11. The spatial distribution is reached by scanning over the FoV with the 2-axis rotation stage. The related angles are so-called α and φ.

Results at 1218.3 Å are illustrated in figure 10 while results at 1356 Å are illustrated in figure 11.
No sharp variation is observed. Anyway, the response is not uniform :
At 1218.3 Å, response is varying between 6 and 12 counts/s for 1000 photons/s/cm²
At 1356 Å, response is varying between 5 and 12 counts/s for 1000 photons/s/cm².

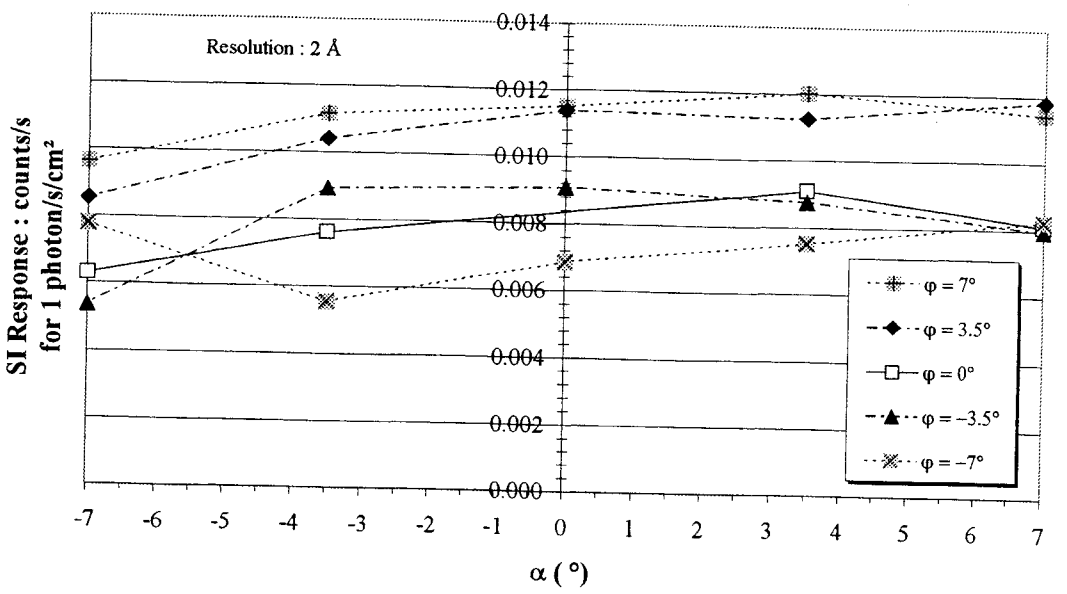

Figure 10 : SI Response at 1218.3 Å for 24 field angles.

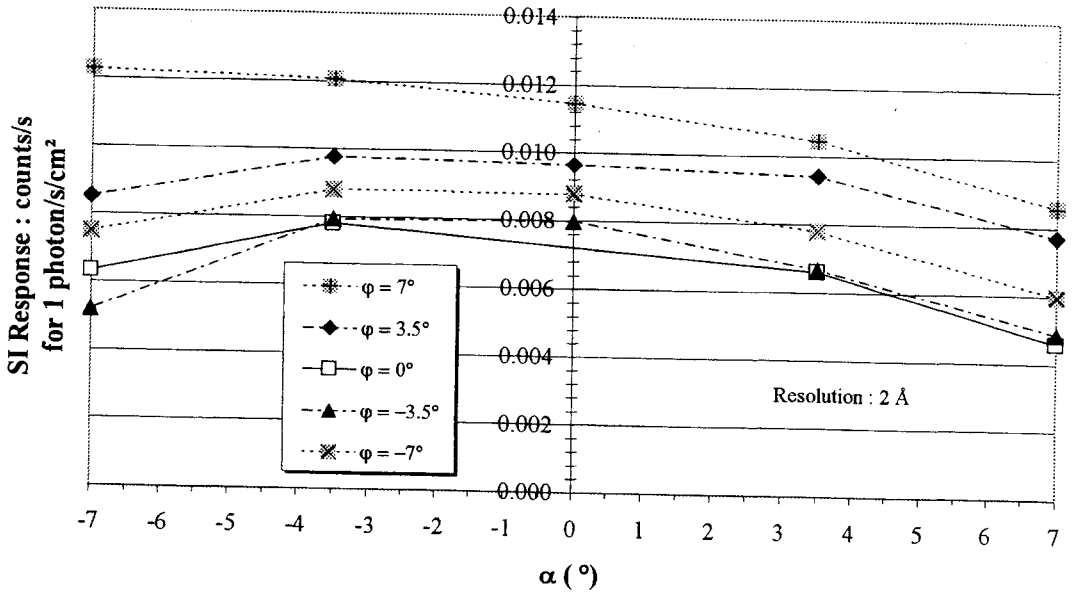

Figure 11 : SI Response at 1356 Å for 24 field angles.

4. CONCLUSIONS

A procedure for Field of View calibration was described. It allows for accurate angular measurements with respect to the optical reference cube mounted on the instrument only (absolute referential, not related to external axis).
Correlation with the point spread function centroid give rise to the image position knowledge, FoV borders determination, and distortion matrix.
For TDI purpose, a set of two second-order polynomial fitting was calculated : one polynomial per wavelength channel.
The RMS distortion fitting error is about 1.4 arcmin and the angular resolution is about 5 arcmin x 5 arcmin (FWHM).

The radiometric or response calibration has verified the spectral behavior of the SI and its sensitivity.
A detailed study of the SI spectrum in the 1200-1400 Å bandwidth was presented. It proofs that the SI is responding at the correct wavelength and that it is blind to emission lines for which it was designed. Actually, the experimental profile is in very good agreement with the theoretical profile.
The wavelength was determined with a precision of ±0.25 Å in the 1170-1270 range and ±0.5 Å in the 1300-1400 range.
The sensitivity was measured with a precision of about 20%.
It appears that the 1218 Å channel seems to be slightly more sensitive than the 1356 Å one :

- the average SI response at 1218.3 Å is 9.0 counts/s for 1000 photons/s/cm² (standard deviation = 2.0)
- the average SI response at 1356 Å is 8.2 counts/s for 1000 photons/s/cm² (standard deviation = 2.1)

Comparisons between both channels are hard to perform with a satisfactory accuracy :

- the 1356 Å channel has one more reflective surface
- the grating blazed angle is optimized for 1216 Å
- the slit grill transmission is slightly higher at 1356 Å (no exit slit grill !)
- the detector window transmission is better at 1356 Å
- the detector photocathode features a higher QE at 1218 Å

Compensation occurs and, finally, the sensitivity is quite similar on both channels.
As mentioned on §3.1., the estimation of loss factor and the knowledge of the SI sensitivity should be correlated. The overall transmission was estimated at about 7% at 1218.3 Å and 1356 Å. The SI aperture surface is 1.27 cm².
We find good correlation when the detector photocathode QE is about 10% at 1218 Å and 9 % at 1356 Å. This is a satisfactory order of magnitude.

The FoV dependence of the SI response was measured. Reasons for such a dependence were detailed on this paper. We can conclude that the SI has a smooth dependence over the FoV. The ratio between the highest and lowest response is about 2.

ACKNOWLEDGMENTS

This work was supported by ESA under ESTEC Contract N° 12328/97/NL/US.

REFERENCES

1. S. Habraken, C. Jamar, P. Rochus, S. Mende, and M. Lampton, "Optical Design of the FUV Spectrographic Imager for the IMAGE Mission," *EUV, X-Ray, and Gamma-Ray Instrumentation for Astronomy VIII*, O.H.W. Siegmund and M.A. Gummin, ed., Proc. SPIE **3114**, 544-553 (1997).
2. S. Habraken, Y. Houbrechts, E. Renotte, C. Jamar, S. Mende, H. Frey, and O. Siegmund, "Alignment and Performances of the FUV Spectrographic Imager for the IMAGE Mission," *EUV, X-Ray, and Gamma-Ray Instrumentation for Astronomy IX*, O.H.W. Siegmund and M.A. Gummin, ed., Proc. SPIE **3445**, 416-426 (1998).
3. E. Renotte, S. Habraken, and P. Rochus, "Design and Verification of the FUV Spectrographic Imager for the IMAGE Mission," *EUV, X-Ray, and Gamma-Ray Instrumentation for Astronomy IX*, O.H.W. Siegmund and M.A. Gummin, ed., Proc. SPIE **3445**, 427-438 (1998).
4. J. Stock, "Crossed-delay-line microchannel plate detector for the spectrographic imager on the IMAGE satellite," *EUV, X-Ray, and Gamma-Ray Instrumentation for Astronomy IX*, O.H.W. Siegmund and M.A. Gummin, ed., Proc. SPIE **3445**, 407-414 (1998).

* Correspondence : Email : shabraken@ulg.ac.be ; http://www.ulg.ac.be/cslulg/ ; Tel. (32) 4-3676668 ; Fax (32) 4-3675613